Accepted Manuscript

Identification of cisapride as new inhibitor of putrescine uptake in *Trypanosoma cruzi* by combined ligand- and structure-based virtual screening

R.C. Dietrich, L.N. Alberca, M.D. Ruiz, P.H. Palestro, Carrillo C, A. Talevi, L. Gavernet

PII: S0223-5234(18)30128-4

DOI: 10.1016/j.ejmech.2018.02.006

Reference: EJMECH 10183

To appear in: *European Journal of Medicinal Chemistry*

Received Date: 28 September 2017

Revised Date: 30 January 2018

Accepted Date: 3 February 2018

Please cite this article as: R.C. Dietrich, L.N. Alberca, M.D. Ruiz, P.H. Palestro, C. C, A. Talevi, L. Gavernet, Identification of cisapride as new inhibitor of putrescine uptake in *Trypanosoma cruzi* by combined ligand- and structure-based virtual screening, *European Journal of Medicinal Chemistry* (2018), doi: 10.1016/j.ejmech.2018.02.006.

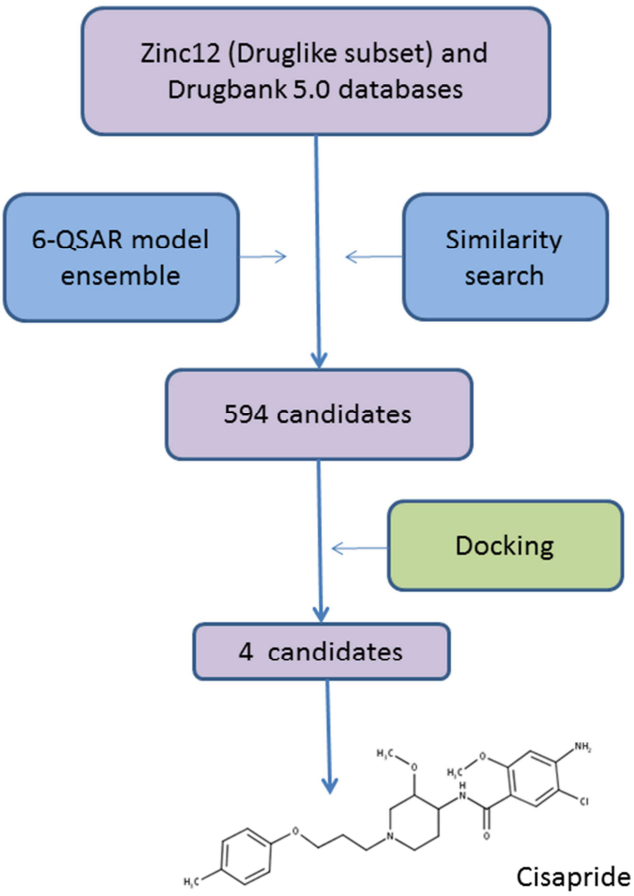

Identification of cisapride as new inhibitor of putrescine uptake in *Trypanosoma cruzi* by combined ligand- and structure-based virtual screening

Dietrich R.C,[a] Alberca L.N,[a] Ruiz M.D.[b], Palestro P.H.[a], Carrillo C[b], Talevi A.[a], Gavernet L.[a].

[a] Laboratorio de Investigación y Desarrollo de Bioactivos (LIDeB), Departamento de Ciencias Biológicas, Facultad de Ciencias Exactas, Universidad Nacional de La Plata, Argentina, 47 & 115, B1900AJI La Plata, Buenos Aires, Argentina.
[b] Instituto de Ciencias y Tecnología Dr. Cesar Milstein (ICT Milstein), Argentinean National Council of Scientific and Technical Research (CONICET), Buenos Aires, Argentina.

Abstract. Nowadays, the pharmacological therapy for the treatment of Chagas disease is based on two old drugs, benznidazole and nifurtimox, which have restricted efficacy against the chronic phase of the illness. To overcome the lack of efficacy of the traditional drugs (and their considerable toxicity), new molecular targets have been studied as starting points to the discovery of new antichagasic compounds. Among them, polyamine transporter *Tc*PAT12 (also known as *Tc*POT1.1) represents an interesting macromolecule, since polyamines are essential for *Trypanosoma cruzi*, the parasite that causes the illness, but it cannot synthesize them de novo. In this investigation we report the results of a combined ligand- and structure-based virtual screening for the discovery of new inhibitors of *Tc*PAT12. Initially we filtered out ZINC and Drugbank databases with similarity and QSAR models and then we submitted the candidates to a validated docking based screening. Four structures were selected and tested in *T. cruzi* epimastigotes proliferation and two of them, Cisapride and [2-(cyclopentyloxy)phenyl]methanamine showed inhibitory effects. Additionally, we performed transport assays which demonstrated that Cisapride interferes with putrescine uptake in a specific mode.

Keywords Chagas disease, Drug repositioning, Cisapride, QSAR, Docking, *Tc*PAT12, *Tc*POT1.1.

1. Introduction.

According to paleoparasitological data, American trypanosomiasis (also known as Chagas disease) is an illness as old as the human presence in the Americas [1]. It was first described by Carlos Chagas more than a century ago [2] and it remains endemic to twenty one Latin America countries [3]. Additionally, population of other regions (such as Canada, United States, Western Pacific and Europe countries) recently started suffering from the disease, mainly due to migratory movements of infected patients [3].

Multi-country initiatives and control campaigns supported by international organisms such as the World Health Organization have substantially reduced the incidence of American trypanosomiasis in the last fifteen years. However, there are still about 7 million people worldwide infected with *Trypanosoma cruzi*, the parasite that causes the disease [3].

Regarding the pharmacological treatment, only two trypanocidal drugs are currently used: benznidazole and nifurtimox. They are effective in the initial, acute phase of the disease but they show limited efficacy against the chronic stage of the infection [4-5]. During such stage the parasites are located mainly in the heart and digestive muscles; and patients can suffer from serious affections on the heart, digestive system and/or, in particular clinical conditions, nervous system [4]. The lack of efficacy of the traditional drugs for the treatment in the chronic phase of the disease in adults and their substantial toxicity explain the need of new active compounds for the treatment of the disease. Interesting advances have been made in this direction, mainly based on the ever growing knowledge of the molecular biology and the biochemistry of *T. cruzi*.

Numerous molecular targets in the parasite have been studied as possible points of intervention with therapeutic objectives. These macromolecules have the common characteristic of being determinants for the parasite survival and/or proliferation, but they are absent (or at least considerably different) in the mammalian host [6]. Among them, in this investigation, we have focused on the polyamine transporter *Tc*PAT12 [7] (also known as *Tc*POT1.1 [8]) as a potential target for the treatment of Chagas disease. This permease, with orthologous sequences in other protozoan parasites such as *Leishmania* spp., *Plasmodium* spp., and *Trypanosoma brucei*, belongs to the amino acid/auxin family (AAAP family), a group of permeases with no homology in the mammalian lineage [9]. Since polyamines are essential for cell survival, differentiation, proliferation and infection of *T. cruzi* [10-11] but it cannot synthesize them *de novo* [12-13], the inhibition of the polyamine uptake prevents the parasite cycle progression [14-15], showing the potential of *Tc*PAT12 as a new therapeutic target for Chagas disease.

Here, we report a search strategy for new putative inhibitors of the transporter *Tc*PAT12 by the implementation of a virtual screening (VS) campaign. We have selected a sequential approach that involves an initial searching with ligand-based filters followed by the application of a target-based method to decide the best candidates. As result, we have tested four compounds, and two of them showed interesting results in epimastigote proliferation, one of them affecting the *Tc*PAT12 activity.

2. Materials and methods

2.1 Ligand-based methods for VS

The initial strategy for the selection of candidates was based on the analysis of known inhibitors. It is worth mentioning that the number of compounds that interact with *Tc*PAT12

reported in literature is scarce. There are few studies about the effect elicited by several small structures over polyamine incorporation in *T. cruzi* cells [16-18]; such information was used for the selection of query molecules to be used in molecular similarity-based searches and for the construction of the validation set for docking calculations.

We started the VS campaign with ligand-based similarity filters. FP2 fingerprints and Tanimoto coefficient were employed for the quantification of molecular similarities; both were calculated by Open Babel 2.3.2 software [19]. Agmatine, Paroxetine, Triclabendazole, Sertaconazole, Pentamidine and Carbonyl cyanide m-chlorophenylsydrazone were used as molecular queries. The selection of the queries was based on the information compiled from literature. The compounds mentioned before display inhibition of the putrescine transport in the micromolar range of concentration [16-18].

One of the major drawbacks of similarity-based methods is their dependency on the input molecules. To overcome this restriction we complemented the similarity-based VS with a recently reported ensemble of QSAR classifiers capable of identifying polyamine analogs with anti-protozoal activity [18].

2.2 Protein structure modeling and docking study

We implemented standard computational strategies to construct tridimensional models of *Tc*PAT12, since its experimental structure is not yet available. The transporter sequence was taken from Uniprot database [20] (accession code B2CQQ7) and it was employed to find the best fitting templates among known 3D structures. By means of Blast server [21] we identified the arginine/agmatine antiporter (AdiC) from *E. coli* (Protein data bank [22] accession code: 3L1L) as the most suitable template. This experimental structure was also selected as template by the other authors who previously proposed 3D models of the transporter [23-24].

The final models were constructed using GPCR-I-TASSER server [25] and Modeller software [26-28]. Among the models achieved for the target, we selected for docking calculations the one with the highest score obtained from Modeller software.

The selection of the docking protocol for VS was based on their capacity to discriminate known inhibitors from non-inhibitors of *Tc*PAT12 through the docking score. For this purpose, we collected from literature those compounds that were tested as inhibitors of the polyamine transportation by *in vitro* models [16-18] and we simulated their interaction with the target by docking (see Table 1 in *Results and Discussion* section). The set of active compounds included the structures previously employed for similarity search and other two molecules, 2,4-dinitrophenol and N-Ethylmaleimidine, which evidenced inhibition at millimolar range of concentration [16]. The criterion for the inclusion of these two structures was to increase the number of active compounds in the test set.

Autodock 4.2 [29] and Autodock Vina [30] software were evaluated by means of both rigid and flexible modes. The “docking active site“ was defined based on previous investigations that

proposed the location of the putrescine-binding pocket [23]. It includes Gly69, Cys66, Trp241, Ala244, Asn145, Cys396, Asn245, Tyr148, Tyr400 amino acids [23].

During Autodock4.2 calculations we set the default spacing (0.375 A) in a grid with 44x58x40 grid points in x, y, z directions. Additionally, we performed the standard estimation for all the variables such as Marsilli-Gasteiger partial charges. We computed 100 docking runs for each compound, with the rotation of all non-ring torsion angles. In the case of flexible dockings, the same parameters and conditions were considered but adding these standard calculations for the mobile residues.

A similar protocol was implemented for Autodock Vina. It has been proposed that this docking software has a better performance over Autodock both in speed and accuracy [30]. However, we tested both softwares because they have different scoring functions, and their accuracy is highly dependent of the ligand-target system under study [31]. In this case we kept a similar grid size as for Autodock, and the standard grid spacing. The number of docking runs was set to 20 for each compound, allowing the rotation of their non-ring torsion angles. We also enabled mobile residues to compare the performance with the rigid model and with Autodock runs. The results are given in *Results and Discussion* section.

2.3 Virtual screening

The similarity search was conducted on Drugbank 5.0 [32] and Zinc12 [33] databases. Drugbank compiles 8,261 compounds, which are mostly experimental drugs (6,000 structures) and also contains nutraceuticals (94 compounds) and FDA-approved drugs (2,021 FDA-approved small drugs and 233 FDA-peptide drugs). To discover *Tc*PAT12 inhibitors from this set of structures would lead to a drug repositioned for this new indication, with all the advantages that drug repositioning holds regarding the optimization of time and resources involved in the process of drug development. Zinc12 database was used to expand the number of chemical scaffolds as well as the number of structures for the screening. We selected its Druglike subset that comprises 17,900,742 purchasable compounds [33]. As mentioned before, the templates for similarity searching were Agmatine, Paroxetine, Triclabendazole, Sertaconazole, Pentamidine and Carbonyl cyanide m-chlorophenylhydrazone. The screening was performed using Open Babel 2.3.2 software. We set a similarity threshold value of 0.5 for Drugbank. In case of ZINC a more demanding filter was established (threshold value 0.7) due to the bigger size of the database.

A parallel ligand-based search was performed with the 6-QSAR model ensemble [18]. We employed an ensemble of the six best previously reported individual models, using the minimum operator to obtain the final score. Such ensemble was applied in the VS using a score of -0.1457 as the threshold value to discern inhibitors from non-inhibitors. Further information can be found in the original report [18].

The resulting hits were submitted to the structure-based VS step, using the *Tc*PAT12 homology model described in section 2.2. An illustration of the VS screening protocol can be visualized in Figure 1.

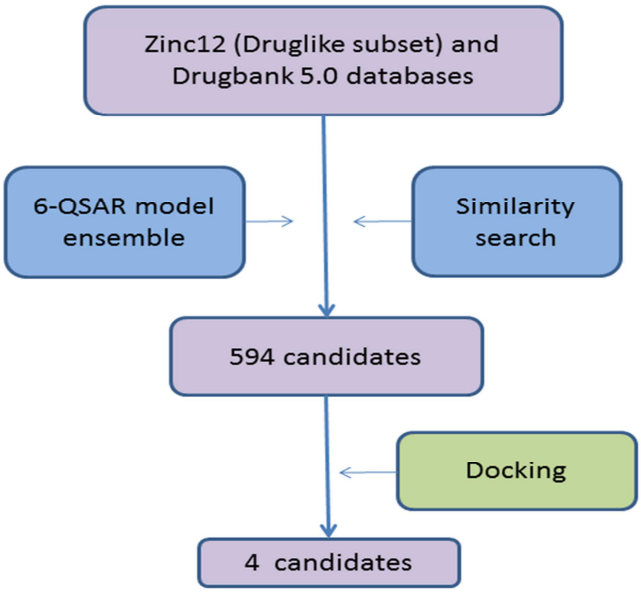

Figure 1. Schematic illustration of the VS protocol used in this investigation.

2.4 Biological Assays

2.4.a- Inhibitory effects on *T. cruzi* epimastigote proliferation. Epimastigotes of the *T. cruzi* strain Y were cultured at 28°C with slightly shaking in BHT medium supplemented with 20 mg/L hemin (Sigma), 10% (v/v) heat-inactivated fetal calf serum (Natocor) and antibiotics (100 µg/mL streptomycin and 100 U/mL penicillin) [18] adding each one of the selected candidate compounds at 0 – 200 µM on 0.1% DMSO. The tested candidate compounds were Cisapride (a gastroprokinetic agent) from Saporiti, and three purchasable amines: ±1-(2,6-Dimethylphenoxy)-2-propanamide (also known as Mexiletine, Compound **1**) from Sigma Aldrich), and 4-(3-(1,3-benzodoxol-5-yloxy) propyl-methyl-amino) cyclohexyl) methanol (Compound **2**) and [2-(cyclopentyloxy)phenyl]methanamine (Compound **3**) from Enamine. Benznidazole (Sigma Aldrich) was used as a reference proliferation inhibitor.

Cultures were initiated at 10^6 cells/mL, and proliferation was followed by periodically cell counting in a hemocytometer chamber. In order to compare the effect of each treatment, at least three independent experiment were used to determine the parameters maximum cell density at seventh day of culture, and IC_{50} (concentration that inhibited 50% of parasite proliferation), evaluated by regression analysis of the data with GraphPad Prism 5 Software.

2.4.b- Compounds effect on putrescine uptake. The inhibitory effect of the selected compounds on putrescine uptake was determined as previously reported [18]. Briefly: Aliquots of *T. cruzi* epimastigotes ($3x10^7$ parasites) grown for 6 h in a polyamine depleted medium were centrifuged at 1500g for 4 min and washed three times with phosphate-buffered saline (PBS). The cells were then resuspended in 2 mL of PBS containing 5 μM [^{14}C]-putrescine and the selected compounds, or putrescine as isotopic displacement control, at a final concentration of 50 μM on 0.1% DMSO. To stop the reaction, aliquots were taken at the indicated times and washed twice by centrifugation with 1 mL of ice-cold PBS and 10 mM putrescine, for isotopic dilution. Pellets were resuspended and radioactivity determined in UltimaGold XR. Similar procedure was followed using 5 μM [1,4-^{14}C]-arginine instead of [^{14}C]-putrescine, in order to check the specificity of compounds effect on putrescine uptake [34].

Possible toxic effects of candidate compounds on the epimastigotes under uptake assay conditions were discarded by the 3-(4,5-dimethyl-thiazol-2-yl)-2,5-di-phenyltetrazolium bromide (MTT) assay (Sigma Aldrich), following the supplier's instructions. In this assay it is determined the capacity of the cell to convert MTT to an acidic isopropanol-soluble blue formazan derivative detected by absorbance at 570 nm.

All assays were made in duplicate and statistical analysis was performed in GraphPad Prism 5 Software. Groups were analyzed using one-way ANOVA test followed by a post-hoc Dunnett's multiple comparison test (significance cut-off value p= 0.05).

3. Results and Discussion

3.1 Virtual screening

The ligand-based VS of the databases identified 594 candidates, which were selected for the target-based VS. These compounds showed either similarity with some of the queries used in the similarity-based VS or were classified as active by the QSAR model-ensemble.

The best model of *Tc*PAT12 architecture was achieved by Modeller Software (Figure 2A), which employed the 3D structure of arginine/agmatine antiporter (AdiC) from *E. coli* as template. These results are in concordance with previous predictions of the structure of the transporter, which were based on the same template [23-24]. It was identified through Blast sequence search from Chimera software [35]. AdiC showed 23% of sequence identity and 64% coverage of the entire query sequence. The model is composed by 12 transmembrane domains with a region of helical discontinuity. The model includes the sequence portion between amino acids 45 and 514 and contains the putrescine-binding pocket (that is, the region needed for docking calculations). The residues uncovered belong to the C- and N-terminus of the transporter. Figure 2B shows a comparison between the putative ligand binding site of the transporter and the crystal structure of the AdiC arginine binding pocket. The architecture of the proposed binding site is similar to the one previously suggested by Hasne and coworkers [23]. As these authors explained before, the α-amino group of arginine

interacts through hydrogen bonds with Ile23, Trp202 and Ile205 in AdiC and these residues are Cys66, Trp241 and Ala244 in the parasite transporter (Figure 2B1). The structural differences between the natural ligands (arginine for AdiC and polyamines for *Tc*PAT12) explain the dissimilarities found in the nature of the residues of the binding sites. For example, the carboxylate group of arginine promotes a hydrogen bonding interaction with the hydroxyl group of Ser26 in the prokaryotic antiporter, whereas this position is occupied by Gly69 in the model of the polyamine transporter (Figure 2B2) [23]. Additionally, the interaction of the guanidine function of arginine with Asn101 and Ser357 in AdiC is partially lost in *Tc*PAT12 model, where the residues are replaced by Asn145 and Cys396 respectively [23]. We also found important residues proposed by Hasne as places of interaction with the polyamine ligands, which are not conserved in AdiC. They are Asn245, Tyr148 and Tyr400 (Figure 2B1) [23].

Ramachandran plot obtained from the model (Figure A1 in Supporting Information section) shows that the backbone dihedral angles are mainly distributed in allowed regions (96%), and none of the residues located in non-allowed regions were involved in the active site of the transporter. Even it is known that the structural characteristics of membrane proteins (such as atomic interactions and solvation properties) do not follow the same distribution as proteins in solution [36], the quality of the model was also estimated with the normalized Discrete Optimized Protein Energy parameter (z-DOPE) and the GA341 score (which analyze the reliability of a model based on statistical potentials) [37]. The values were 0.8 for z-DOPE and 0.723 for GA341. These results showed that the model has an acceptable reliability (given by GA341 values higher than 0,7) but the z-DOPE score is higher than expected (negative values indicate better models). The z-DOPE value was calculated based on native structures of macromolecules and may be biased towards globular proteins that may not follow the same distribution values for structural properties as those from membrane proteins. Therefore we decided to use the model for virtual screening based on the Ramachandran plot results and the fact that it is able to reproduce the position and orientation of key residues of the binding site mentioned previously in the text [23].

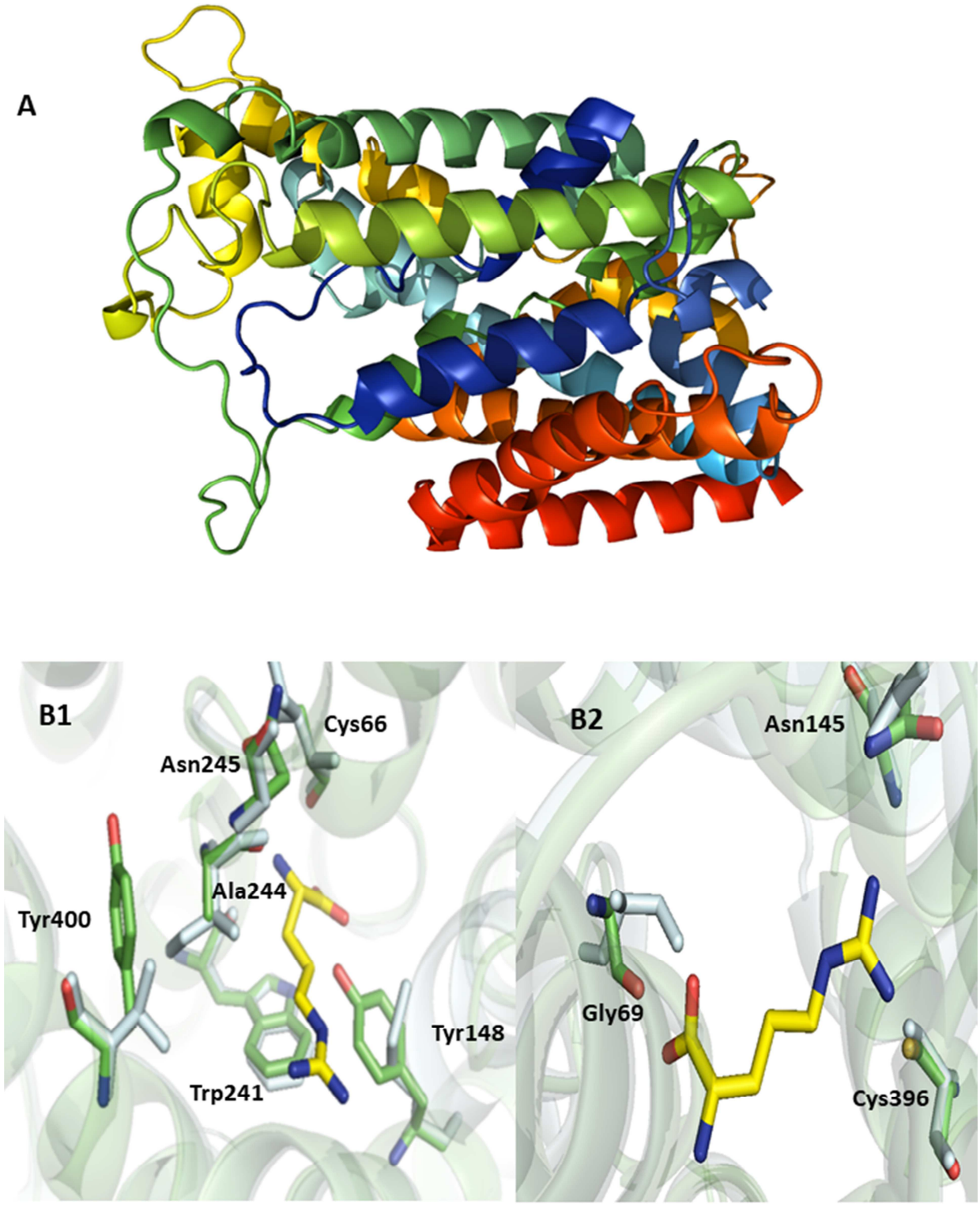

Figure 2. The three-dimensional model of *Tc*PAT12 architecture used for virtual screening. A: side view of the model. B: Superposition of the putative binding site of the model (in green) and AdiC binding pocket (in cyan). Important residues of *Tc*PAT12 model are highlighted as sticks with the following color code: carbon atoms in green, oxygen atoms in red, nitrogen atoms in blue and sulfur atoms in yellow. The corresponding amino acids of AdiC were

highlighted as cyan sticks. Arginine ligand of AdiC has carbon atoms in yellow. B1: residues predicted to be involved in polyamine recognition B2: Important residues that interacts with carboxylic and guanidine function of the ligand in AdiC and the corresponding residues in *Tc*PAT12.

The docking protocol for VS was selected by considering the capacity of the docking software to identify known active compounds. As mentioned before, the information available in literature refers to several small molecules that interfere (or not) in the process of polyamines uptake in *T. cruzi* cells. Table 1 shows the scores achieved by the simulation of the interaction of these molecules with the target, through the execution of different docking protocols. 2,4-dinitrophenol, Agmatine, Paroxetine, Carbonyl cyanide m-chlorophenylhydrazone, Triclabendazole, N-Ethylmaleimidine, Sertaconazole, and Pentamidine were reported as inhibitors of the polyamine transport whereas Spermine and the amino acids Aspartate, Asparagine, Lysine and Serine were considered non-inhibitors [16-18]. The natural ligands of the transporter (cadaverine and putrescine) were also included within the validation set.

For Autodock 4.2 we considered *Tc*PAT12 as a rigid structure in the first model (M1, Table 1). Additionally three different set of amino acids of the active site were allowed to move in the Autodock flexible docking simulations (M2 to M4, Table 1). The criterion of selection of the mobile residues was based on the analysis of the amino acids that interact with the natural ligands (cadaverine and putrescine) in the rigid simulations. We found hydrogen bonding interactions between the ligands and Glu247 (Figure A2 in Supporting Information section). Additionally, Tyr148 pointed its hydroxyl group to one amino moiety of the ligands, so both aminoacids were considered flexible in order to optimize these of interactions (M2). Asn145 was also included as flexible with the same criteria (M4). Finally Trp241 and Ala244 side chains were allowed to move in order to analyze the effect of possible hydrophobic interactions (M3). Similarly, we performed docking calculations with Autodock Vina software (models M5 to M8, Table 1).

Autodock Vina simulations calculated lower scores for the inhibitors than reference ligands showing their ability to identify them as active compounds. Models M6, M7 and M8 recognized 100% of the inhibitors with a lower score than putrescine and cadaverine. However, these simulations assigned also lower scores to non-inhibitors and they were able to identify only one non inhibitor through the docking score.

Table 1. Docking scores for the test set. Flexible residues are included between brackets. Inactive compounds are shown in italic. Amino acids were docked in their L and D configurations, only the best docking score is reported in the table. Reference ligands are shown in bold.

Compound	**M1** (rigid)	**M 2** (Glu247 Tyr148)	**M 3** (Glu247 Tyr148 Trp241 Ala244)	**M 4** (Glu247 Tyr148 Asn245)	**M 5** (rigid)	**M 6** (Glu247 Tyr148)	**M7** (Glu247 Tyr148 Trp241 Ala244)	**M8** (Glu247 Tyr148 Asn245)
2,4-dinitrophenol	-5.5	-10.3	-13.3	-9.6	-7.0	-7.6	-7.2	-6.9
Agmatine	-6.6	-13.5	-15.1	-12.1	-5.2	-5.7	-5.6	-5.7
Paroxetine	-9.0	-16.0	-17.6	-14.6	-4.3	-7.9	-7.9	-8.0
Carbonyl cyanide m-chlorophenylhydrazone	-7.1	*-12.2*	-14.3	-10.7	-7.1	-7.3	-7.7	-7.3
Triclabendazole	-8.1	-13.1	-15.4	-11.4	-3.5	-5.5	-7.4	-5.2
N-Ethylmaleimidine	-4.8	*-10.0*	-11.7	-8.2	-5.2	-5.3	-5.4	-5.4
Sertaconazole	-9.4	-15.8	-17.3	-15.7	-3.3	-5.8	-7.6	-5.7
Pentamidine	-9.3	-15.1	-17.6	-12.8	-5.5	-7.9	-8.6	-8.1
Cadaverine	**-5.9**	**-12.6**	**-14.2**	**-10.8**	**-4.1**	**-4.6**	**-4.6**	**-4.6**
Putrescine	**-6.0**	**-11.7**	**-13.3**	**-10.3**	**-3.8**	**-4.4**	**-4.4**	**-4.4**
Spermine	*-7.1*	*-14.1*	*-15.0*	*-12.6*	*-5.4*	*-5.9*	*-6.0*	*-5.9*
Aspartate	*-5.5*	*-10.4*	*-13.0*	*-8.7*	*-5.1*	*-5.2*	*-5.2*	*-5.2*
Asparagine	*-5.7*	*-12.1*	*-14.7*	*-9.6*	*-5.3*	*-5.4*	*-5.6*	*-5.4*
Leucine	*-5.8*	*-11.3*	*-13.6*	*-9.8*	*-5.3*	*-5.2*	*-5.2*	*-5.2*
Lysine	*-8.0*	*-14.2*	*-16.4*	*-12.6*	*-5.0*	*-5.6*	*-5.7*	*-5.7*
Serine	*-5.5*	*-11.8*	*-13.9*	*-10.1*	*-4.4*	*-4.3*	*-4.3*	*-4.2*

The models based on Autodock4.2 simulations showed an acceptable ability to identify inhibitors. M1 and M3 were able to detect most of the inhibitors through their score (75% of them, in relation to the reference ligands). Additionally, M1 showed about 70% of non-inhibitors correctly classified. This specificity in the validation set is important to reduce the selection of false positives in VS, even at expenses of losing some true positives during the search (M1 displays a sensibility rate lower than Autodock Vina models). We also tested the docking conditions recently reported by Reigada and coworkers for VS [24]. The authors considered Asn245, Tyr148 and Tyr400 as flexible residues and performed the simulations using Autodock4.2 software. We applied this model to our test set (M9) and a similar protocol

with Autodock Vina software (M10). The results evidence lower performances than M1 in terms of specificity. Table S1 shows the results achieved from M9 and M10 and Table S2 shows the percentage of false-positives, false-negatives, true-positives and true-negatives for all simulations.

As an additional validation of the M1 model, we tested its capacity to reproduce the experimental binding mode of the complex between Arginine and the Arginine/Agmatine antiporter (AdiC) from *E. coli*, the template selected for the construction of the *Tc*PAT12. The results are shown in Figure 3.

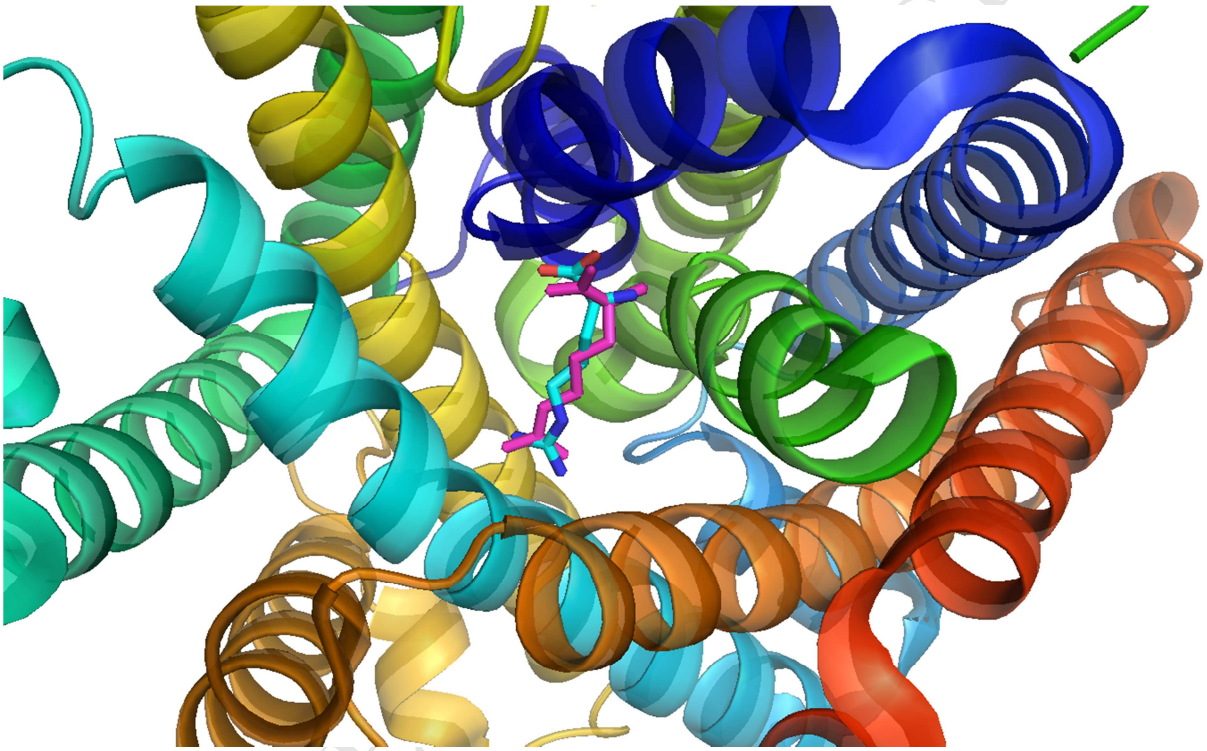

Figure 3. Superposition of the docking conformation (in magenta) and the crystallographic ligand (in light blue) in the active site of AdiC (PDB code 3L1L). Hydrogen atoms were omitted for simplicity.

The results previously mentioned, based on the information of true inhibitors and no inhibitors, allowed us to select M1 as the best docking protocol for the target-based conducting the VS.

The performance of M1 in a VS context was analyzed by constructing a ”simulated database” that contains a set of presumed active compounds dispersed in a large number of apparent inactive structures. To this end, we defined as active putrescine, cadaverine and the inhibitors collected from literature as active (Table 1). Additionally, we increased the number of putative inhibitors through the inclusion of the 25 polyamide analogs with activity towards T. Cruzi

found in literature [18]. These polyamide analogs were previously considered as active for the construction of the QSAR model included in this investigation [18]. On the other hand, we judge as inactive the noninhibitors of the test set (Table 1) and 411 decoys generated with the Enhanced Directory of Useful Decoys resource (DUD-E) [38]. The decoys were calculated from the smiles codes of the active molecules used for similarity searching (Agmatine, Paroxetine, Triclabendazole, Sertaconazole, Pentamidine and Carbonyl cyanide m-chlorophenylsydrazone) plus putrescine and cadaverine. The performance of M1 over the simulated database was tested through the area under the Receiving Operating Characteristic (ROC) curve. It plots the sensibility of the model (true positive rate) as a function of the false positive rate (1−specificity) at predefined threshold settings [39]. The area under the curve (AUC) will be equal to 1 in an ideal performance while an AUC of 0.5 will represent a random selection of active and inactive compounds through the docking scores. The AUC value calculated for M1 was 0.71, which represents a moderate predictive capacity. To the extent of our knowledge previous docking based virtual screening campaigns against TcPAT12 did not report this metric, so we cannot compare our AUC value with the one obtained from other researchers. Finally we measured the enrichment of inhibitors among the top-ranking scores of the simulated database through the enrichment factor (EF) [40]. We found an EF value of 4 for the first 10% of the database. The metrics exposed the moderate performance of the model, and future investigations will be carried out to improve it as new active compounds are identified by us as well as by other authors.

According to the docking scores achieved in the simulated database, we set a cutoff value −7.7 Kcal/mol to differentiate active from inactive compounds in the ‘‘real‘‘ VS. This value was chosen to balance specificity (70%) and sensibility (61%), according to the ROC curve.

From the 594 structures selected from the ligand-based filters, the target-based VS proposed 203 candidates that pass the threshold value. The 59 compounds that comprise the top 10% of the scores were analyzed. Finally, based on their chemical diversity and accessibility, four of them, Cisapride (a gastroprokinetic agent), and three purchasable amines: ±1-(2,6-Dimethylphenoxy)-2-propanamide (Compound **1**), 4-(3-(1,3-benzodoxol-5-yloxy) propyl-methyl-amino) cyclohexyl) methanol (Compound **2**) and [2-(cyclopentyloxy)phenyl]methanamine (Compound **3**) were purchased and tested through *in vitro* assays of *T. cruzi* epimastigote proliferation and polyamine transport (Figure 4).

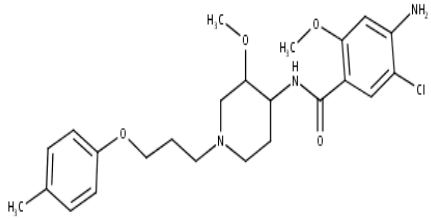

Cisapride

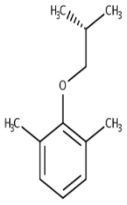

1

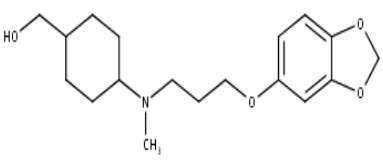

2

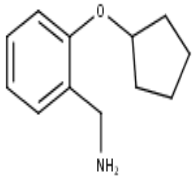

3

Figure 4. Candidates acquired for biological testing.

3.2 Biological Assays

3.2.a- Inhibitory effects on *T. cruzi* epimastigote proliferation

The four selected compounds were tested in proliferation assays on epimastigotes, the proliferative and non-infective stage of *T. cruzi*. Curves without compound addition and with benznidazole were also done as controls. This *in vitro* assay is a first approach to evaluate the possible effect of a compound as trypanocidal or trypanostatic drug.

Comparing with control growth curves, compounds **1** and **2** did not exhibit inhibitory activity, even at high concentration (200 μM), while 60 μM Cisapride and 100 μM Compound **3** diminished significantly the maximum cell density ($p < 0.05$) in the first round of culture (Figure 5A, B and E), showing IC_{50} values of 39.7 μM and 41.1 μM respectively. The Cisapride effect was observed in a concentration range of 30 – 60 μM; at lower (up to 20 μM) and higher concentrations (from 100 μM) the effect progressively disappeared. There are multiple possible explanations to such loss of effect at high concentrations, including Cisapride forming micelles or precipitating in the culture medium. We have found no evidences in the literature on Cisapride forming micelles (aside, its molecular structure does not resemble a surfactant to exhibit such behavior). We did not observe precipitation of the compound in culture medium up to 400 μM,either. Accordingly, we hypothesize that the observed loss of effect at concentrations similar to 100 μM could be a result of induced efflux or elimination, activated once that the compound concentration overcomes certain level.

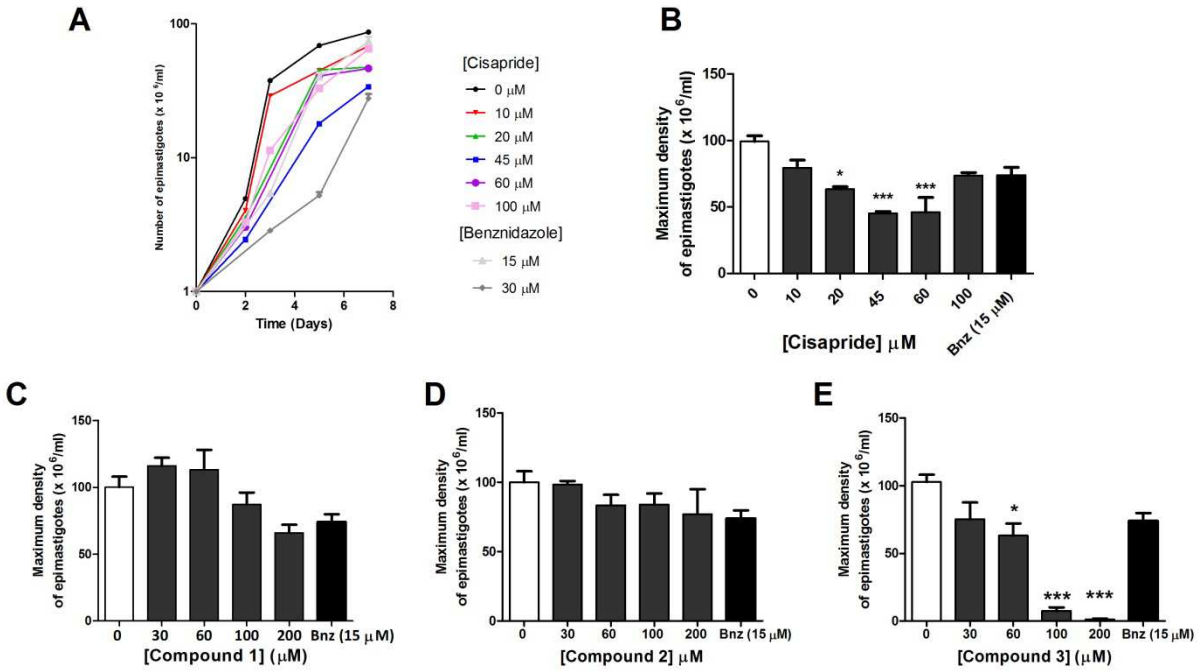

Figure 5. Evaluation of candidate compounds in *in vitro* epimastigotes proliferation assay. To follow growth curves and determine maximum cell density at each condition, epimastigotes, strain Y, were seeded at 10^6 cells/ml in BHT medium and maintained at 28 C°. Parasites were counted periodically using a hemocytometer chamber. Control condition (0 μM) was tested at 0.1% DMSO. **A)** Growth curves of epimastigotes treated with Cisapride or Benznidazole at different concentrations, illustrating maximum cell density values obtained at the 7th day of culture. One of three independent experiments with similar results is shown. **B – E)** Effect of candidate compounds on maximum cell density reached at the 7th day (first round of culture). Cisapride (B), Compound 1 (C), Compound 2 (D), Compound 3 (E). Values are expressed as mean ± SD. Statistical analysis was performed by one way ANOVA test followed by a post-hoc Dunnett's multiple comparison test, considering 0 μM as control mean (*$p < 0.05$, **$p < 0.01$, ***$p < 0.005$).

3.2.- Compounds effect on putrescine uptake

In order to check if the candidate compounds interfere with putrescine uptake, as predicted by our models, we evaluated their competition capacity in a [^{14}C]-putrescine transport assay in *T. cruzi* epimastigotes. The maximal uptake interference was obtained by an isotopic displacement control done with non-radioactive 50-fold molar putrescine (not shown). Cisapride, at 10-fold molar excess, showed a clear effect on putrescine uptake with a significant initial velocity reduction to 53 ± 5.2% (Figure 6A), compared with transport in control conditions. In contrast, putrescine uptake was not affected by Compounds **1**, **2** and **3** (Figure 6A).

The specificity of the inhibitory effect caused by Cisapride on putrescine uptake was checked by two different kinds of experiments: by competition assays on Arginine transport, whose permease *Tc*AAAP411 belongs to the same family of *Tc*PAT12, the AAAP family [9,34], and by evaluation of possible toxicity effect under transport conditions.

There was no effect of Cisapride on Arginine uptake (Figure 6A, inset – maximal displacement effect showed by non-radioactive arginine, not shown) indicating that the observed effect on putrescine transport was specific rather than an unspecific effect on AAAP members. Complementarily, Compound **3** also was tested for competition on Arginine uptake, confirming that its negative effect on epimastigote proliferation was not related with the uptake of putrescine nor arginine. On the other hand, it was performed a MTT assay under conditions and times of the uptake assay allowing us to discard that the observed effect on putrescine uptake with Cisapride was due to compound cytotoxicity (Figure 6B). These results indicate that the Cisapride effect was specific on putrescine uptake.

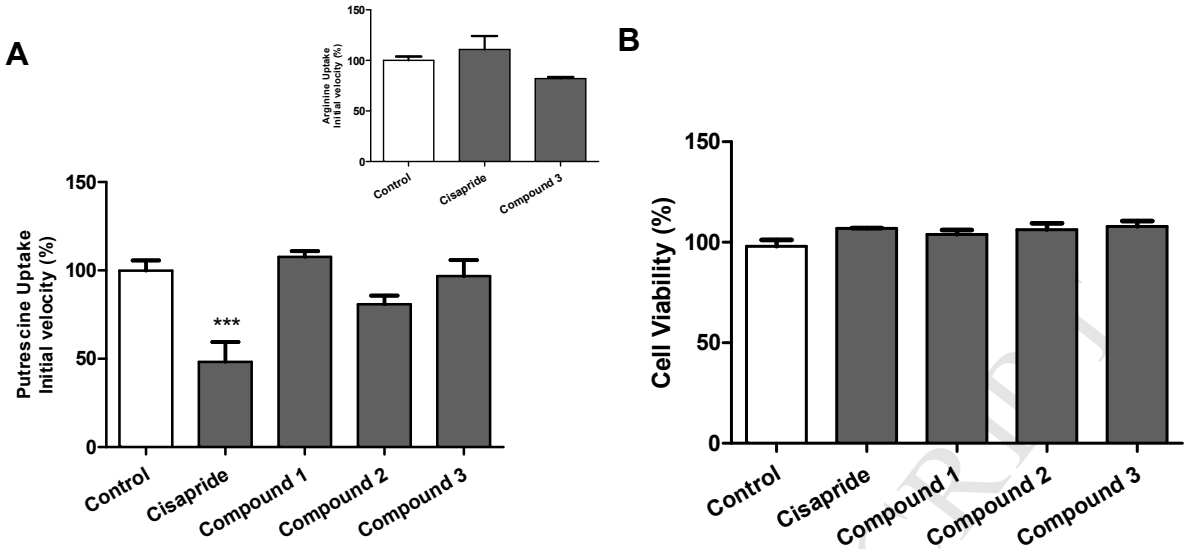

Figure 6. Effect of Cisapride and compounds **1**, **2** and **3** on putrescine uptake in *T. cruzi* epimastigotes. A- Competition Assay: early log parasite cultures were harvested for 6 hs in a polyamine free medium. Then putrescine uptake was assayed at 5 µM [^{14}C]-putrescine and initial velocities were calculated at 0.1% DMSO (control condition) and adding 250 µM non-radioactive putrescine (maximal interference – not shown) or 50 µM of each candidate compound. Values are expressed as % mean ± SD with in comparison with control. Statistical analysis was performed by one way ANOVA test followed by a post-hoc Dunnett's multiple comparison test (***$p < 0.005$). Inset: competition assays on Arginine uptake were realized with same cultures and conditions with 5 µM [1,4-^{14}C]-Arginine in order to check the specificity of compounds effect. B- Viability assay: the metabolic state of the epimastigote cells was evaluated by the MTT assay, where tetrazolium salt is reduced to a alcohol-soluble blue formazan product determined by Absorbance at 570nm.

4 Conclusions

We have performed a cascade VS campaign by combining parallel similarity and QSAR ligand-based VS with subsequent target-based screening of the resulting hits.

Four of the hits selected *in silico* were acquired and screened both in *T. cruzi* epimastigotes proliferation and putrescine uptake assays. Two of the assayed hits, Cisapride and 2-(cyclopentyloxy)phenyl]methanamine (Compound **3**), displayed inhibitory effects on epimastigote proliferation. In the case of Cisapride, it was verified that this drug interferes with putrescine uptake in a specific manner (without impairing arginine uptake or cell viability), while no effect on putrescine uptake was observed for Compound **3**. The verified effect of Cisapride on putrescine uptake confirms the ability of our cascade *in silico* screen to select compounds targeting polyamine uptake.

It should be underlined that the trypanocidal effects of Cisapride seem to be lost at high concentrations, which may be explained through an induced efflux. Future studies should assess if such loss at high concentrations is also observed in *T. cruzi* clinically relevant forms (trypomastigotes and amastigotes), in order to evaluate the potential of Cisapride as starting point for the development of new medications against Chagas disease.

5. Acknowledgments

The authors would like to thank the following public and non-profit organizations: National University of La Plata and Exact Sciences Faculty, Argentinean National Agency of Scientific and Technical Research (ANPCyT), PICT 2013-0520, CONICET. PIP 0664/13 - CONICET

6. References

(1) L.F. Ferreira, A.M. Jansen, A. Araújo A., Chagas disease in prehistory. An Acad. Bras. Cienc. 83 (2011) 1041–1044.
(2) C. Chagas, Nova tripanozomiase humana: Estudos sobre a morfolojia e o ciclo evolutivo do Schizotrypanum cruzi n. gen., n. sp., ajente etiolojico de nova entidade morbida do homem, Mem. Inst. Oswaldo Cruz 1 (1909) 159–218.
(3) World Health Organization. Research Priorities for Chagas Disease, Human African Trypanosomiasis and Leishmaniasis, WHO Technical Report Series 975 (2012) 11-14.
(4) P. Veiga-Santos, K. Li, L. Lameira, T.M. Ulisses de Carvalho, G. Huang, M. Galizzi, N. Shang, Q. Li, D. Gonzalez-Pacanowska, V. Hernandez-Rodriguez, G. Benaim, R.T. Guo, J.A. Urbina, R. Docampo, W. de Souza, E. Oldfield, SQ109, a New Drug Lead for Chagas Disease, Antimicrob. Agents Chemother. 59 (2015) 1950-1961.
(5) C.A. Morillo, J.A. Marin-Neto, A. Avenzum, S. Sosa-Estani, A. Rassi, F. Rosas, E. Villena, R. Quiroz, R. Bonilla, C. Britto, F. Guhl, E. Velazquez, L. Bonilla, B. Meeks, R. Rao-Melacini, J. Pogue, A. Mattos, J. Lazdins, A. Rassi, S.J. Connolly, S.J.; Yusuf, S. Randomized trial of benznidazole for chronic Chagas' cardiomyopathy, N. Engl. J. Med. 373 (2015) 1295–1306.
(6) J.M. Bustamante, R.L. Tarleton, Potential new clinical therapies for Chagas disease, Expert Rev. Clin. Pharmacol. 7 (2014) 317-325.
(7) C. Carrillo, G.E. Canepa, I.D. Algranati, C.A. Pereira, Molecular and functional characterization of a spermidine transporter (TcPAT12) from Trypanosoma cruzi, Biochem Biophys Res Commun. 344 (2006) 936-40.
(8) M.P. Hasne, I. Coppens, R. Soysa, B. Ullman, A high-affinity putrescine-cadaverine transporter from Trypanosoma cruzi, Mol Microbiol. 76 (2010) 78-91.
(9) L.A. Bouvier, A.M. Silber, C. Galvão Lopes, G.E. Canepa, M.R. Miranda, R.R. Tonelli, W. Colli, M.J. Alves, C.A. Pereira, Post genomic analysis of permeases from the amino acid/auxin family in protozoan parasites. Biochem Biophys Res Commun. 321 (2004) 547-56.
(10) J.J. Barclay, L.G. Morosi, M.C. Vanrell, E.C. Trejo, P.S. Romano, C. Carrillo, Trypanosoma cruzi Coexpressing Ornithine Decarboxylase and Green Fluorescence Proteins as a Tool to Study the Role of Polyamines in Chagas Disease Pathology, Enzyme Res. 2011, (2011) 657460.
(11) M.C. Vanrell, J.A. Cueto, J.J. Barclay, C. Carrillo, M.I. Colombo, R.A. Gottlieb, P.S. Romano, Polyamine depletion inhibits the autophagic response modulating *Trypanosoma cruzi* infectivity, Autophagy 9 (2013) 1080-1093.
(12) M.R. Ariyanayagam, A.H. Fairlamb, Diamine auxotrophy may be a universal feature of Trypanosoma cruzi epimastigotes, Mol Biochem Parasitol. 84 (1997) 111-21.
(13) C. Carrillo, S. Cejas, N.S. González, I.D. Algranati, Trypanosoma cruzi epimastigotes lack ornithine decarboxylase but can express a foreign gene encoding this enzyme. FEBS Lett. 454 (1999) 192-6.
(14) C. Reigada, M. Sayé, E.V. Vera, D. Balcazar, L. Fraccaroli, C. Carrillo, M.R. Miranda, C.A. Pereira, Trypanosoma cruzi Polyamine Transporter: Its Role on Parasite Growth and Survival Under Stress Conditions, J Membr Biol. 249 (2016) 475-481.
(15) M.P. Hasne, R. Soysa, B. Ullman, The Trypanosoma cruzi Diamine Transporter Is Essential for Robust Infection of Mammalian Cells, PLoS One. 2016, 11:e0152715.

(16) S.A. Le Quesne, A.H. Fairlamb, Regulation of a high-affinity diamine transport system in Trypanosoma cruzi epimastigotes, Biochem. J. 316 (1996) 481–486.
(17) M.V. Díaz, M.R. Miranda, A. Campos-Estrada, C. Reigada, J.D. Maya, C.A. Pereira, R. López-Muños, Pentamidine exerts in vitro and in vivo anti Trypanosoma cruzi activity and inhibits the polyamine transport in Trypanosoma cruzi, Acta Tropica 134 (2014) 1–9.
(18) L.N. Alberca, M.L. Sbaraglini, D. Balcazar, L. Fraccaroli, C. Carrillo, A. Medeiros, D. Benitez, M. Comini, A. Talevi, Discovery of novel polyamine analogs with anti-protozoal activity by computer guided drug repositioning J. Comput. Aided Mol. Des. 30 (2016) 305-32.
(19) N.M. O'Boyle, M. Banck, C.A. James, C. Morley, T. Vandermeersch, G.R. Hutchison, Open Babel: An Open chemical toolbox. Journal Cheminform. 3 (2011) 33.
(20) The UniProt Consortium. UniProt: the universal protein knowledgebase, Nucleic Acids Res. 45 (2017) D158-D169.
(21) S.F. Altschul, W. Gish, W. Miller, E.W., Myers, D.J. Lipman, Basic local alignment search tool, J. Mol. Biol. 215 (1990) 403-410.
(22) Z. Feng, G. Gilliland, T.N. Bhat, H. Weissig, I.N. Shindyalov, P.E. Bourne, H.M. Berman, J Westbrook, The Protein Data Bank, Nucleic Acids Res. 28 (2000) 235-242.
(23) R. Soysa, H. Venselaar, J. Poston, B. Ullman, MP Hasne, Structural model of a putrescine-cadaverine permease from Trypanosoma cruzi predicts residues vital for transport and ligand binding, Biochem. J. 452 (2013) 423–432.
(24) C. Reigada, E.A. Valera-Vera, M. Sayé, A.E. Errasti, C.C. Avila, R. Mariana, M.R. Miranda, C.A. Pereira, Trypanocidal Effect of Isotretinoin through the Inhibition of Polyamine and Amino Acid Transporters in Trypanosoma cruzi, PLoS Negl Trop Dis 2017, 11(3): e0005472.
(25) J. Zhang, J. Yang, R. Jang, Y. Zhang, GPCR-I-TASSER: A hybrid approach to G protein-coupled receptor structure modeling and the application to the human genome, Structure 23 (2015) 1538-1549.
(26) M. Martí-Renom, A. Stuart, Comparative Protein Structure Modeling of Genes and Genomes, Annu. Rev. Biophys. Biomol. Struct. 29 (2000) 291–325.
(27) A. Fiser, K.D. Do, A. Sali, Modeling of loops in protein structures. Protein Sci. 9 (2000) 1753-1773.
(28) A. Sali, T.L. Blundell, Comparative Protein Modelling by Satisfaction of Spatial Restraints. J. Mol. Biol. 234 (1993) 779–815.
(29) G.M. Morris, R. Huey, W. Lindstrom, M.F. Sanner, R.K. Belew, D.S. Goodsell, A.J. Olson, Autodock4 and AutoDockTools4: automated docking with selective receptor flexiblity. J. Comput.l Chem. 16 (2009) 2785-2791.
(30) O. Trott, A.J. Olson, AutoDock Vina: improving the speed and accuracy of docking with a new scoring function, efficient optimization, and multithreading, J. Comp. Chem. 31 (2010) 455–461.
(31) D.B. Kitchen, H. Decornez, J.R. Furr, J. Bajorath, Docking and scoring in virtual screening for drug discovery: methods and applications Nat. Rev. Drug Discov. 3 (2004) 935-949.
(32) V. Law, C. Knox, Y. Djoumbou, T. Jewison, A.C. Guo, Y. Liu, A. Maciejewski, D. Arndt, M. Wilson, V. Neveu, A. Tang, G. Gabriel, C. Ly, S. Adamjee, Z.T. Dame, B. Han, Y. Zhou, D.S. Wishart, DrugBank 4.0: shedding new light on drug metabolism, Nucleic Acids Res. 42 (2014) 1091-1097.
(33) J.J. Irwin, T. Sterling, M.M. Mysinger, E.S. Bolstad, R.G. Coleman, ZINC: a free tool to discover chemistry for biology, J. Chem. Inf. Model. 52 (2012) 1757-1768.

(34) C. Carrillo, G.E. Canepa, A. Giacometti, L.A. Bouvier, M.R. Miranda, M.M. Camara, C.A. Pereira, Trypanosoma cruzi amino acid transporter TcAAAP411 mediates arginine uptake in yeasts. FEMS Microbiol Lett. 306 (2010) 97-102.

(35) E.F. Pettersen, T.D.Goddard, C.C. Huang, G.S. Couch, D.M. Greenblatt, E.C.Meng, T.E.Ferrin, UCSF Chimera--a visualization system for exploratory research and analysis. J Comput Chem. 25 (2004) 1605-1612.

(36) P. Benkert, M. Biasini, T. Schwede Toward the estimation of the absolute quality of individual protein structure models. Bioinformatics 27 (2011) 343–350.

(37) F. Melo, R. Sanchez, A. Sali, Statistical potentials for fold assessment Protein Science 11 (2002) 430–448.

(38) M.M. Mysinger, M. Carchia, J.J. Irwin, B.K. Shoichet, Directory of Useful Decoys, Enhanced (DUD-E): better ligands and decoys for better benchmarking. J Med Chem 55 (2012) 6582–6594.

(39) N. Triballeau, F. Acher, I. Brabet, J.P. Pin, H.O. Bertrand, Virtual screening workflow development guided by the ‘‘receiver operating characteristic’’ curve approach. Application to highthroughput docking on metabotropic glutamate receptor subtype 4, J Med Chem 48 (2005) 2534–2547.

(40) A. Bender and R. C. Glen, A discussion of measures of enrichment in virtual screening: Comparing the information content of descriptors with increasing levels of sophistication, J. Chem. Inf. Mod 45 (2005) 1369–1375.

A combined virtual screening was conducted for the discovery of TcPAT12 inhibitors.

A 3D model of the target was constructed for the target based virtual screening.

Transport assays showed that Cisapride interferes with putrescine uptake.